AD-A185 257 REDUCTION OF COLLAPSING LOSS IN REPAIR DISPLAYS(U) 1/1
NAVAL RESEARCH LAB WASHINGTON DC B R JARRETT ET AL.
11 SEP 87 NRL-9057

UNCLASSIFIED F/G 17/9 NL

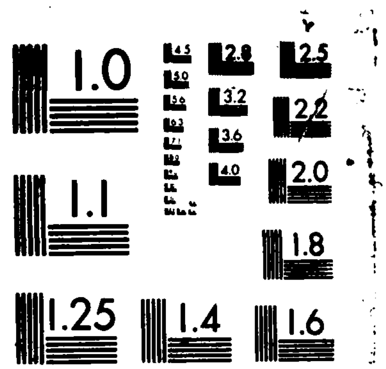

MICROCOPY RESOLUTION TEST CHART
NATIONAL BUREAU OF STANDARDS-1963-A

Naval Research Laboratory
Washington, DC 20375-5000

DTIC FILE COPY

②

NRL Report 9057

AD-A185 257

Reduction of Collapsing Loss in Radar Displays

B. R. JARRETT AND C. L. TEMES

Search Radar Branch
Radar Division

September 11, 1987

AD-A 185 257

SECURITY CLASSIFICATION OF THIS PAGE

REPORT DOCUMENTATION PAGE

1a REPORT SECURITY CLASSIFICATION UNCLASSIFIED	1b RESTRICTIVE MARKINGS
2a SECURITY CLASSIFICATION AUTHORITY	3 DISTRIBUTION / AVAILABILITY OF REPORT Approved for public release; distribution unlimited.
2b DECLASSIFICATION / DOWNGRADING SCHEDULE	
4 PERFORMING ORGANIZATION REPORT NUMBER(S) NRL Report 9057	5 MONITORING ORGANIZATION REPORT NUMBER(S)
6a NAME OF PERFORMING ORGANIZATION Naval Research Laboratory — 6b OFFICE SYMBOL (If applicable) 5334.J	7a NAME OF MONITORING ORGANIZATION
6c ADDRESS (City, State, and ZIP Code) Washington, DC 20375-5000	7b ADDRESS (City, State, and ZIP Code)
8a NAME OF FUNDING / SPONSORING ORGANIZATION Naval Sea Systems Command — 8b OFFICE SYMBOL (If applicable)	9 PROCUREMENT INSTRUMENT IDENTIFICATION NUMBER
8c ADDRESS (City, State, and ZIP Code) Washington, DC 20362-5101	10 SOURCE OF FUNDING NUMBERS

PROGRAM ELEMENT NO	PROJECT NO	TASK NO	WORK UNIT ACCESSION NO
64508N		S0166	DN980-149

11 TITLE (Include Security Classification)
Reduction of Collapsing Loss in Radar Displays

12 PERSONAL AUTHOR(S)
Jarrett, B. R. and Temes, C. L.

13a TYPE OF REPORT	13b TIME COVERED	14 DATE OF REPORT (Year, Month, Day)	15 PAGE COUNT
Final	FROM ______ TO ______	September 11, 1987	23

16 SUPPLEMENTARY NOTATION

17 COSATI CODES			18 SUBJECT TERMS (Continue on reverse if necessary and identify by block number)
FIELD	GROUP	SUB-GROUP	Radar; Collapsing loss
			Plan position indicator; Peak detection/holding

19 ABSTRACT (Continue on reverse if necessary and identify by block number)

A "collapsing loss" occurs when the video output of a radar is displayed on a plan position indicator that has significantly poorer resolution than the radar. In this report we investigate the performance improvement gained by using peak detection/hold circuitry to obtain a pseudoresolution match between the radar and the display, and we develop the appropriate relationship between peak detect/hold interval, spot size, and sweep speed. Analysis of the improvement to be gained through peak detection/holding was obtained by computer simulation, and additional data were obtained by experiment with an AN/SPS-10 radar and an AN/SPA-25 display located at the Chesapeake Bay Detachment of NRL. For linear detection, peak detection/holding appears to promise a considerable gain at significant values of collapsing ratio; the situation for square-law detection is less promising because the losses are lower. The question of whether almost/barely visible radar signals on a display (the case of most interest) correspond more closely to linear or square-law detection is left open; however, the experimental data and other researchers suggest it is normally linear.

20 DISTRIBUTION / AVAILABILITY OF ABSTRACT ☒ UNCLASSIFIED/UNLIMITED ☐ SAME AS RPT ☐ DTIC USERS	21 ABSTRACT SECURITY CLASSIFICATION UNCLASSIFIED
22a NAME OF RESPONSIBLE INDIVIDUAL B. R. Jarrett	22b TELEPHONE (Include Area Code) (202) 767-6947 — 22c OFFICE SYMBOL 5334.J

DD FORM 1473, 84 MAR — 83 APR edition may be used until exhausted. All other editions are obsolete.

SECURITY CLASSIFICATION OF THIS PAGE

*U.S. Government Printing Office: 1985-507-047

CONTENTS

REDUCTION OF COLLAPSING LOSS IN RADAR DISPLAYS

INTRODUCTION

When the video output of a radar is displayed on a plan position indicator (PPI) that has significantly less resolution than the radar, a collapsing loss L_c occurs. In this report we review the extent of the loss and discuss its importance in current and future shipboard systems. We also investigate the performance improvement gained by using peak detection/hold circuitry to obtain a pseudoresolution match between radar and display. Analysis of the improvement to be gained through peak detection/holding is obtained by computer simulation and by experiment by using an AN/SPS-10 radar and AN/SPA-25 display located at the Chesapeake Bay Detachment (CBD) of NRL.

The principal features of the computer-based analysis are: (a) a model for simulating the collapsing loss phenomenon in displays, (b) a Monte Carlo simulation to obtain probability-of-false alarm (P_{FA}) curves for both normal and peak detect/hold cases as a function of threshold value for different collapsing ratios, and (c) a Monte Carlo simulation to obtain probability-of-detection (P_D) curves as a function of signal-to-noise ratio (SNR) for different collapsing ratios, again for both the normal and peak detected/held cases. The simulation was run twice; first using linear and then square-law detection (the amount of loss is influenced by the type of detection).

In the experimental investigation, a digital peak detect/hold circuit with variable peak detect/hold interval was developed and inserted between the radar and display. The peak detect/hold circuit could be switched in and out to enable comparison of detection performance in each mode. PPI photographs provide a visible record of comparative performance.

Thus, the theoretical profile of the loss characteristic was obtained by simulation for both the normal and peak detected/held cases, and a visual indication of the performance improvement was obtained by experimentation using digital peak detection/hold processing.

No attempt was made to obtain simulation data for any conditions other than Swerling Case 0 (nonfluctuating targets) and single-hit P_D.

BACKGROUND

In general, collapsing loss occurs when noise, originating outside the radar-resolution element that contains the signal, is mixed with the signal and the signal's associated noise [1]. In this report we are only interested in the collapsing loss that occurs in displays; however, other causes of collapsing loss include excessive range-gate width, improper receiver bandwidth, and summation of doppler filter banks to a single detector.

Collapsing loss has been defined [2] as the SNR required with M extra noise pulses, when noncoherently integrating N signal-plus-noise pulses, divided by the SNR required with no extra noise

Manuscript approved April 27, 1987.

pulses. The required probabilities of false alarm and detection are the same in both cases. Expressed in dB, the definition is:

$$L_c = 10 \log_{10} \frac{(S/N)_{N+M}}{(S/N)_N}, \tag{1}$$

where $(S/N)_{N+M}$ is the SNR required with N signal-plus-noise and M extra noise pulses, and $(S/N)_N$ is the signal-to-noise ratio required with N signal-plus-noise pulses alone.

In many cases, the integrations required to establish the P_D needed to obtain the required SNRs for Eq. (1) are difficult, and computer simulations or Meyer plots are employed. A parameter called collapsing ratio has generally been used as a first measure of collapsing loss and is needed when using Meyer plots. Meyer plots are not directly applicable in determining collapsing loss for the peak detect/hold case; therefore, Monte Carlo simulation was used to obtain the theoretical loss profile. Collapsing ratio is defined as

$$\rho = \frac{M + N}{N}, \tag{2}$$

where

N is the number of signal-plus-noise samples integrated, and
M is the number of additional noise-alone samples integrated.

Large values of collapsing ratio imply large collapsing loss; when $\rho = 1$ there is no collapsing loss.

CRT CONSIDERATIONS

In a stroke-type PPI, the receiver output intensity modulates the cathode-ray-tube (CRT) beam current [3]. The beam, at any instant in time, illuminates a spot on the CRT screen; each time the radar emits a pulse a trace is produced that travels radially out from the center of the screen. This trace, commonly called a sweep, rotates in synchronism with the antenna (for rotated antennae) and the target returns in a radar beamwidth (dwell) produce the characteristic "banana." It has empirically been determined that the operator usually performs postdetection integration with an integration improvement factor approximately proportional to $n^{1/2}$ where n is the number of pulses in a dwell. The persistence of the screen is longer than the scan time, and there may be some overlap of pulses from consecutive sweeps. This general effect, when viewed by an observer, is also a part of postdetection integration. However, it is not postdetection integration we are interested in per se. Instead, we concentrate on the single sweep (single hit) characteristics of the spot and the integration therein.

A radar range resolution cell can be defined in terms of the pulse width. Pulse duration (length of the signal on the CRT) is the equivalent display parameter. When a radar and display are mismatched, a resolution cell (spot) on the display encompasses a number of radar range resolution cells. In this situation, if a signal (i.e., point target return) exists, it is normally in only one of the cells, the others containing noise alone. From Eq. (2),

$$\rho = \frac{M + N}{N}.$$

With $N = 1$ for our particular case,

$$\rho = M + 1,$$

and $M + 1$ is the number of radar range resolution cells per display spot size. In this idealized concept the shape of the range resolution cells within the spot is not important (they are defined to be of equal area), and the spot can be represented as shown in Fig. 1.

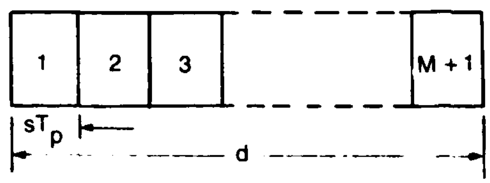

Fig. 1 — Idealized representation of the spot as $M + 1$ range resolution cells

The part of the spot that contains the signal is proportional to the product of the sweep speed s (in./s) and the pulse width T_p (s). Therefore, collapsing ratio could also be defined in this case as

$$\rho = \frac{d}{sT_p}, \tag{3}$$

where d is the radial dimension of the spot. Hence, ρ will change as a function of sweep speed. For example, if $s_2 = s_1/2$, the number of PPI range resolution cells corresponding to s_2 would be twice the number corresponding to s_1 and $\rho_2 = 2\rho_1$. Collapsing loss is, therefore, higher when the PPI is set up to display longer ranges. The effect on detectability is most pronounced when the returns have low SNR. Detectability is further degraded by the fact that the spot size increases, being considerably larger at the periphery of the CRT than it is at the center.

Collapsing loss also occurs in scan-conversion systems that use raster displays. The situations are entirely equivalent, and, indeed, since the resolution of stroke displays is generally better than raster types, an increase in collapsing loss would normally be expected in scan-converted displays.

DESCRIPTION OF THE SIMULATION MODEL

Figure 2 is a block diagram showing the signal and noise generators and the two processors used for comparison of the normal and peak detect/hold cases. The inputs to both processors are identical. The additive noise is obtained from Gaussian distributed noise samples generated from uniformly distributed random numbers by the relationship

$$I_n = \sqrt{-\ln U_1} \cos(2\pi U_2), \tag{3a}$$

where U_1 and U_2 are independent random numbers uniformly distributed on the (0,1) interval. An independent quadrature variable is generated from the same two random numbers by

$$Q_n = \sqrt{-\ln U_1} \sin(2\pi U_2). \tag{3b}$$

The variance, $\overline{I_n^2} + \overline{Q_n^2}$, is one (average noise power is unity).

Figure 2 depicts the integration process within the spot as the summation of the $M + 1$ range resolution cells of Fig. 1. In actuality, the analogy is to an element of screen area da (spot) along a sweep whose intensity output is proportional to the sum of $M + 1$ samples (beams) only one of

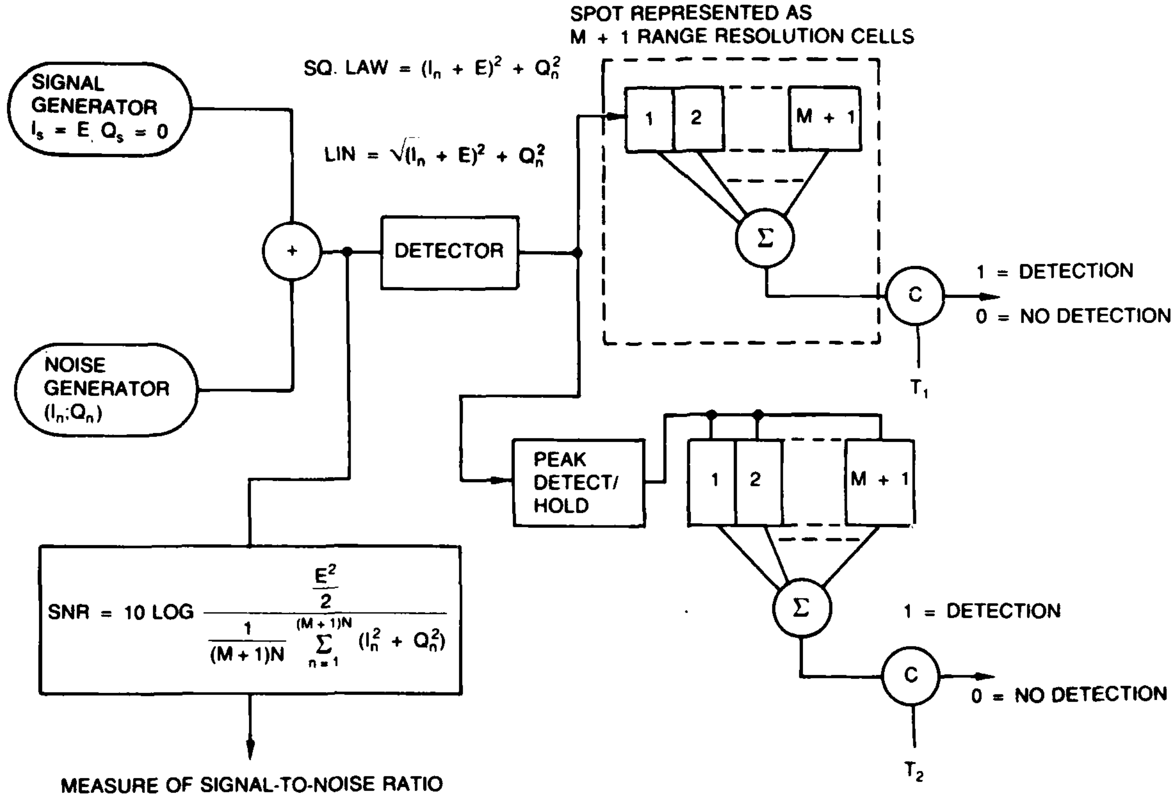

Fig. 2 — Block diagram of Monte Carlo simulation to obtain P_{FA} and P_D

which contains signal. In the same manner, it is convenient to peak detect over $M + 1$ samples and sum $M + 1$ identical values to obtain the signal corresponding to the spot intensity (multiplying the peak value by $M + 1$ produces the same result) for the peak detect/hold case.

LINEAR VS SQUARE-LAW DETECTION

Trunk [4] has shown that collapsing loss is greater for linear detection than for square-law detection.* Blake [5, pp. 2-25,26] states that "appreciable RF and IF gain usually precedes the second detector, so that the voltage applied to it is usually large enough to ensure this linear type of operation. It is important to note that this statement does *not* stipulate a large *signal-to-noise ratio* but, rather, a large *detector input voltage* (relative to the value at which the transition from square-law to linear input-voltage-output-current relationship occurs). Therefore, the second detector of a superheterodyne radar receiver usually operates as a linear detector, even for very small signal-to-noise ratios, or even in the complete absence of a signal, because the noise voltage alone is sufficient to ensure operation in the linear region."

Blake also points out that in a linear rectifier there is a square-law relationship for small SNRs (because of the statistics of the signal-noise superposition) that becomes linear for large SNRs, but the effect is not because of a square-law, voltage-current relationship, and it does not mean that a linear detector becomes a square-law detector for small SNRs.

In the interest of generality, the approach taken is to do the simulation twice, once for square-law and once for linear detection, in order to place bounds on the problem. Note, however, that the

*Helpful discussions with E. Khoury of Business Technological Systems, Inc. on this topic are also acknowledged.

P_D curves to be presented for square-law detection will not be strictly valid, since in any diode detector receiver there would have been a transition to linear operation at some input value, which, as Blake has stated, could be at very small SNRs, even on noise alone. Moreover, it is apparent that the case of most interest is when the SNRs are near those that produce a barely visible signal on the display, and the corresponding improvement that can be gained by means of peak detection/holding. Whether linear or square-law detection is performed in this region or not is a function of the specific radar in question. If we accept Blake's position, it would normally be linear.

SIMULATION RESULTS

In determining detection performance of a receiver by a Monte Carlo simulation one must know the threshold setting that provides a specified P_{FA} [6]. Therefore, the first step in the simulation is to determine the threshold settings T_1 and T_2 as a function of P_{FA} for various collapsing ratios. This is accomplished by setting the input signal to zero and measuring P_{FA} as a function of threshold setting. Figure 3(a) shows a representative example of these results for the normal case, and Fig. 3(b) shows the peak detect/hold case, for a collapsing ratio of 8. The curves are important insofar as they allow us to obtain threshold values for a given P_{FA} to use in determining P_D as a function of SNR.

Using the threshold settings at a P_{FA} value of 10^{-3}, the simulation was then run varying the signal amplitude. Obtaining data for P_{FA}s lower than 10^{-3} does not closely correspond to PPI/operator detection performance. The results are presented in Figs. 4-9 for collapsing ratios of 2, 4, 8, 16, 32, and 64, respectively, where P_D is plotted as a function of SNR. SNR is defined as

$$\mathrm{SNR} = 10 \log \frac{\dfrac{E^2}{2}}{\dfrac{1}{(M+1)N} \displaystyle\sum_{n=1}^{(M+1)N} (I_n^2 + Q_n^2)} \tag{4}$$

where $M + 1$ is the number of samples in the spot as shown in Fig. 1, N corresponds to the Monte Carlo number (the number of times the simulation is run with a new set of noise variates for the spot), and the signal is $E \cos 2\pi f_{if} t$.

For each collapsing ratio, curves are generated for both the normal and peak detect/hold cases, and to facilitate comparison, the curve for $\rho = 1$ (no L_c) is also provided. In each figure, part (a) is for linear detection and part (b) is for square-law detection.

These curves are tabulated in Table 1 to show the loss and recovery data for a number of collapsing ratios for both linear and square-law detection.

Table 1 — Tabulation of Collapsing Loss Data
($P_{FA} = 10^{-3}$)

Collapsing Ratio ρ	Collapsing Loss (dB, approx.)		Recovered by Peak Detection/Holding (dB, approx.)	
	Linear	Sq Law	Linear	Sq Law
2	2.00	0.75	1.50	0.50
4	4.00	2.00	3.50	1.00
8	7.00	2.50	5.50	1.50
16	9.00	4.00	7.50	2.50
32	11.00	5.00	9.00	3.00
64	14.00	6.00	12.00	4.00

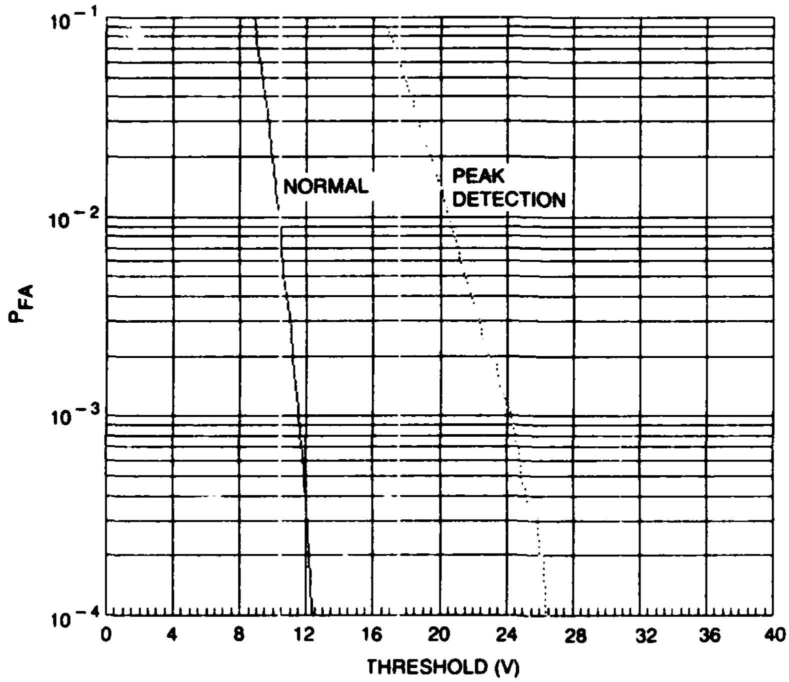

(a)

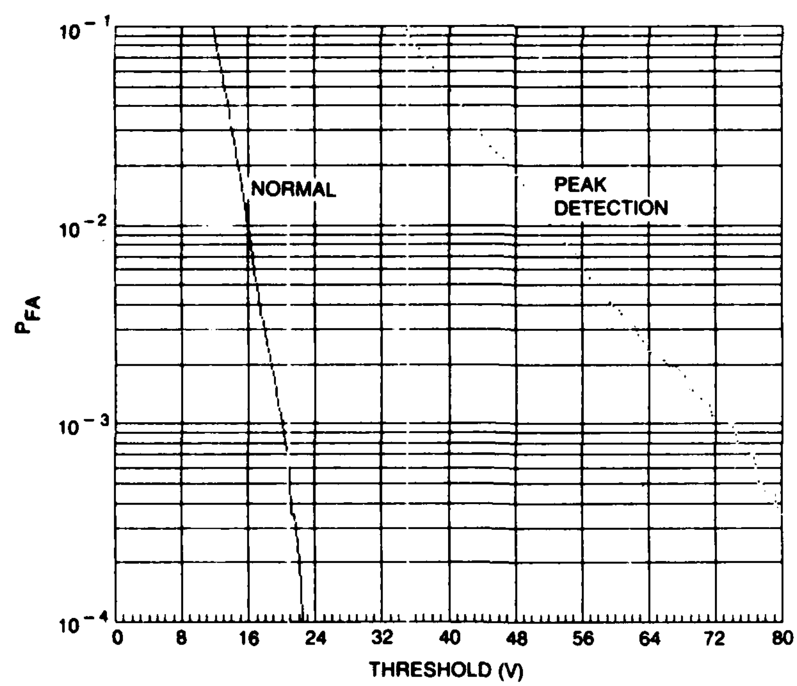

(b)

Fig. 3 — Probability of false alarm (P_{FA}) vs threshold curves for $\rho = 8$; normal and peak-detected cases; for (a) linear and (b) square-law detection

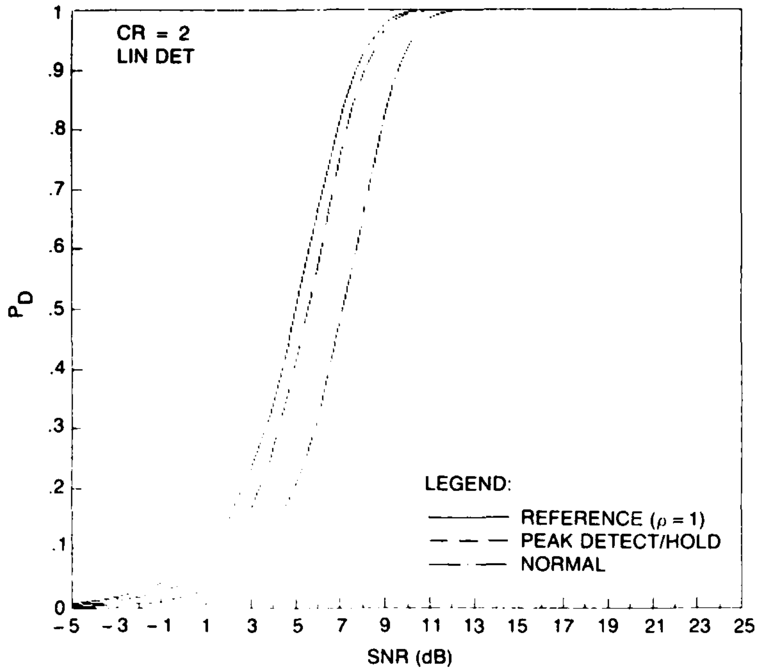

(a)

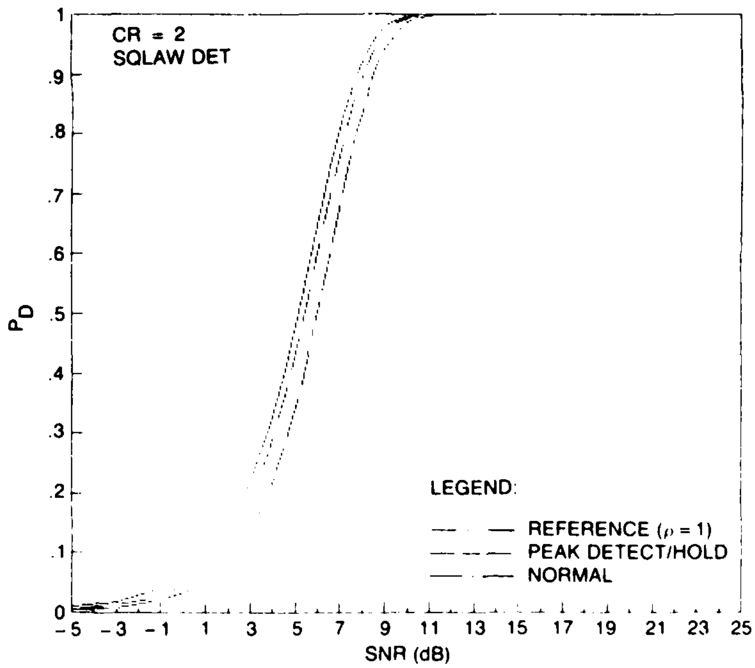

(b)

Fig. 4 — P_D vs SNR, normal and peak detected cases, ρ = 2, referenced to ρ = 1, for (a) linear detection and (b) square-law detection

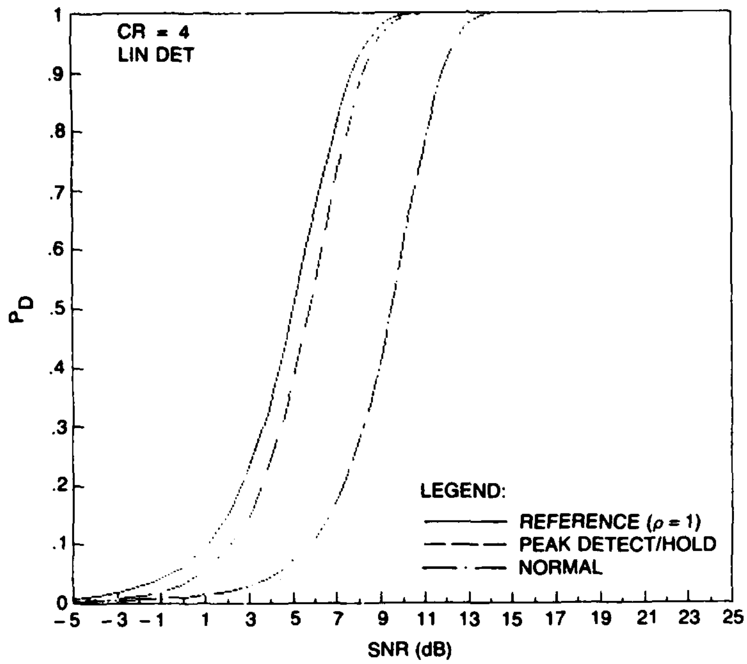

(a)

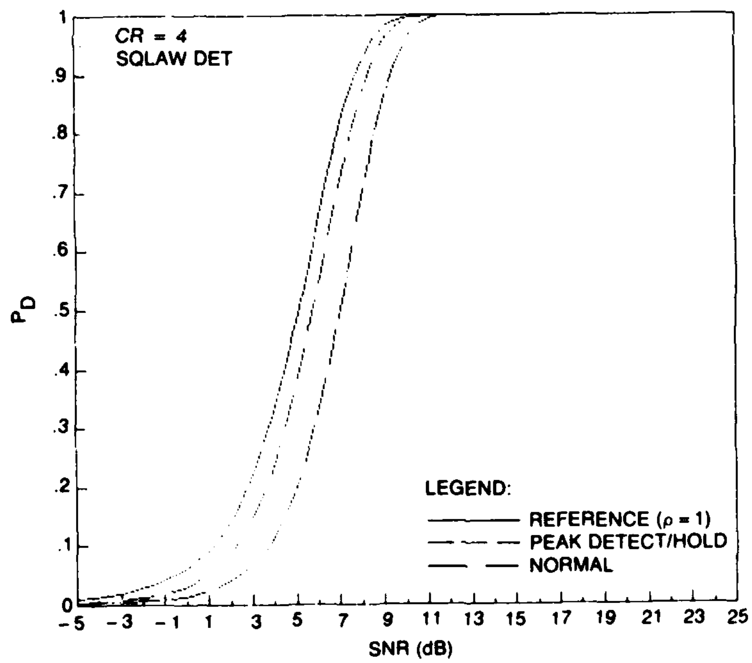

(b)

Fig. 5 — P_D vs SNR, normal and peak detected cases, $\rho = 4$, referenced to $\rho = 1$, for (a) linear detection and (b) square-law detection

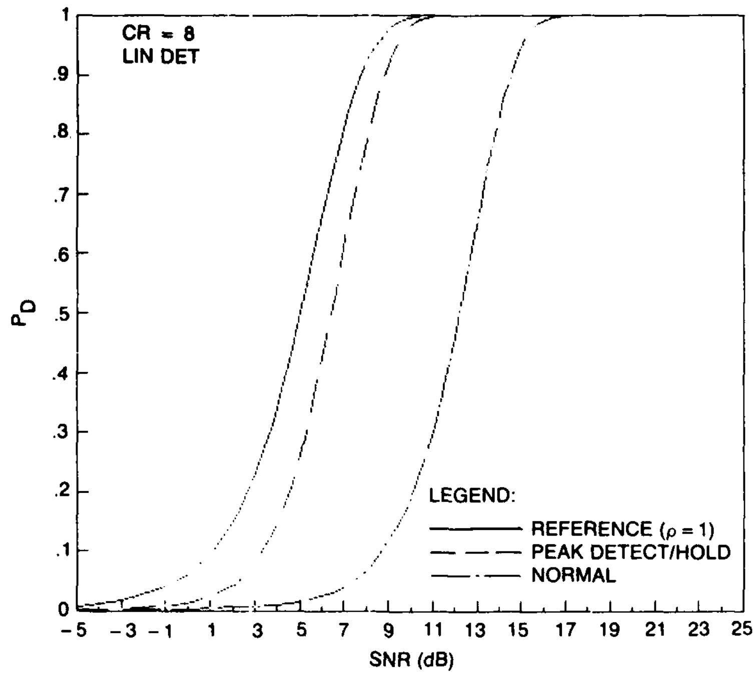

(a)

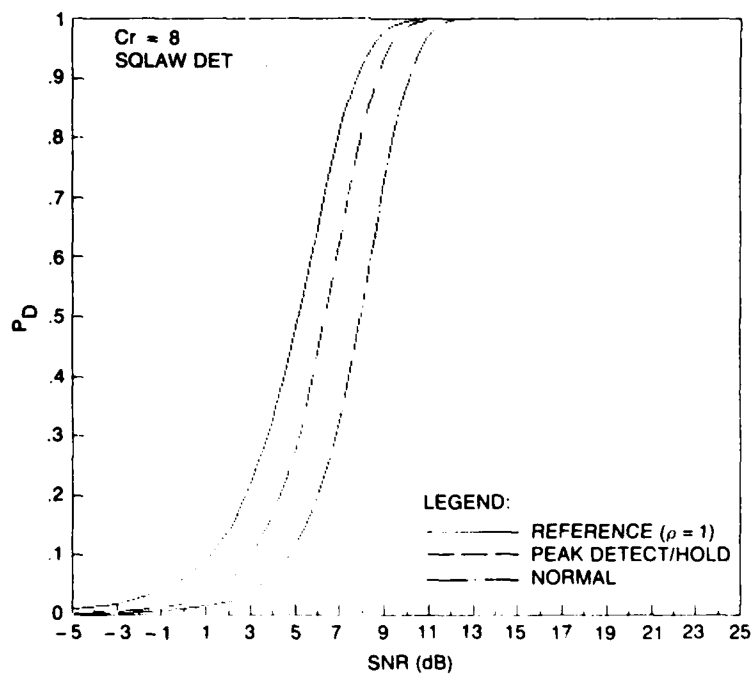

(b)

Fig. 6 — P_D vs SNR, normal and peak detected cases, $\rho = 8$, referenced to $\rho = 1$, for (a) linear detection and (b) square-law detection

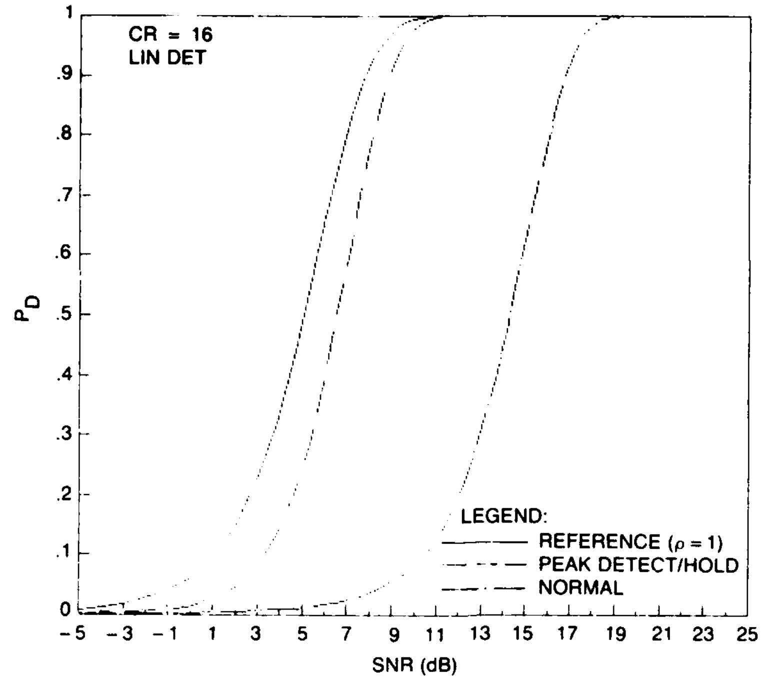

(a)

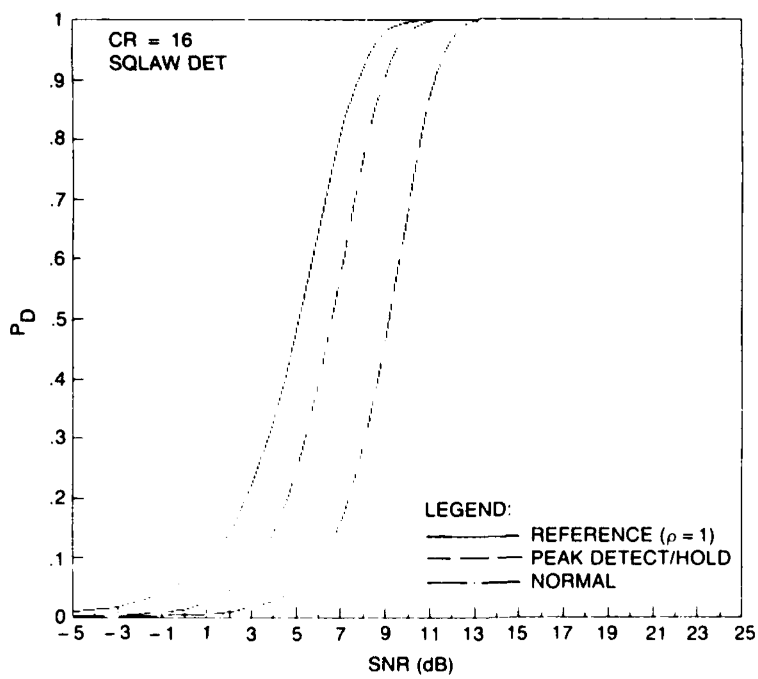

(b)

Fig. 7 — P_D vs SNR, normal and peak detected cases, $\rho = 16$, referenced to $\rho = 1$, for (a) linear detection and (b) square-law detection

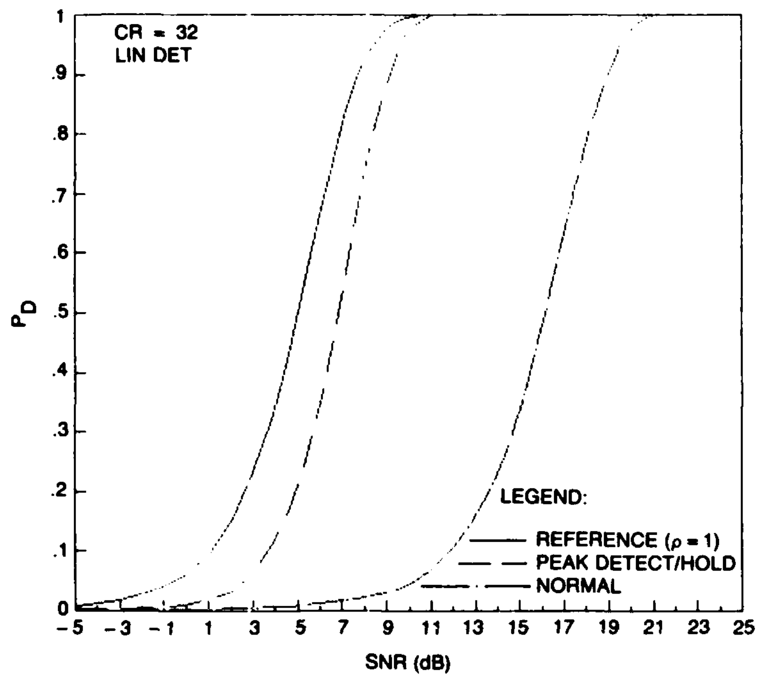

(a)

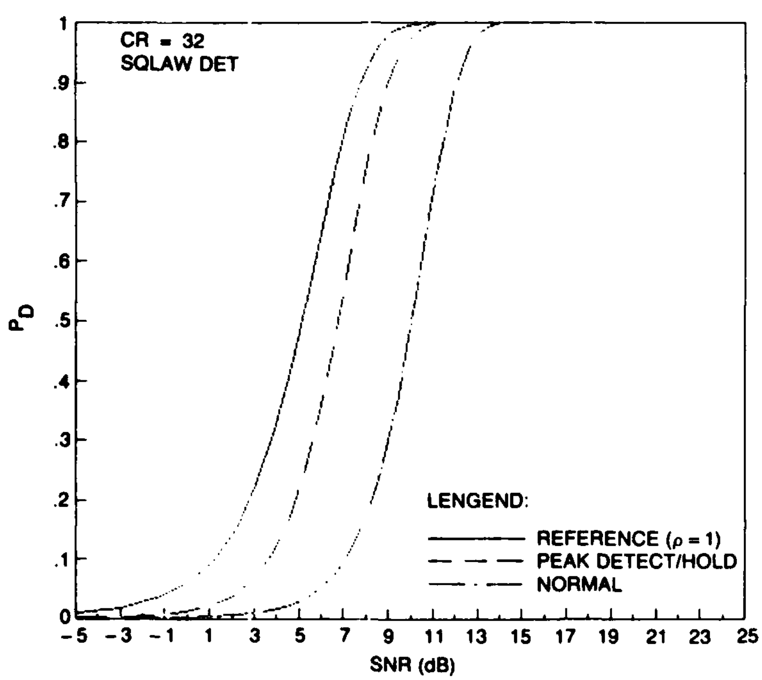

(b)

Fig. 8 — P_D vs SNR, normal and peak detected cases, ρ = 32, referenced to ρ = 1, for (a) linear detection and (b) square-law detection

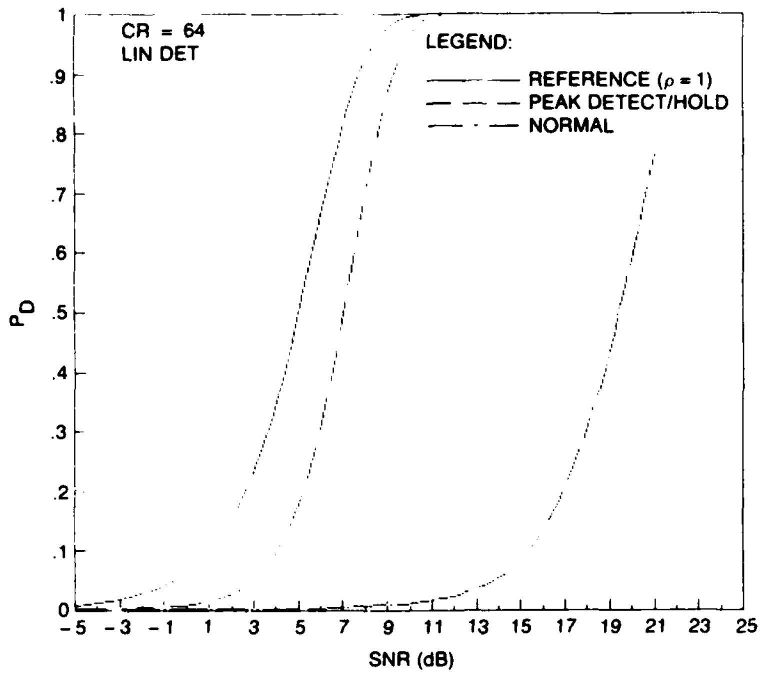

(a)

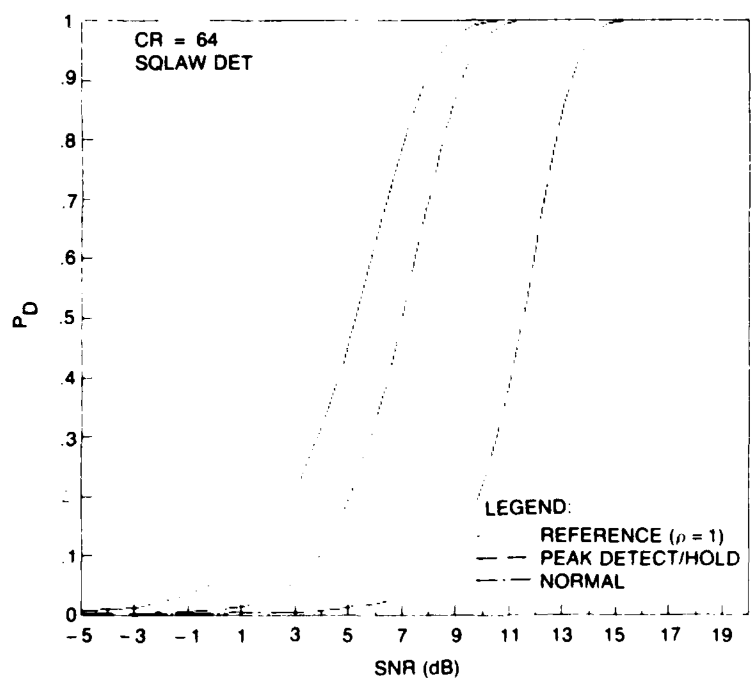

(b)

Fig. 9 — P_D vs SNR, normal and peak detected cases, ρ = 64, referenced to ρ = 1, for (a) linear detection and (b) square-law detection

For linear detection, peak detection/holding appears to promise a considerable gain at significant values of collapsing ratio; indeed, it seems possible to limit the losses to within 2 dB for the range of collapsing ratios that would normally be encountered. This assumes the loss characteristic is not heavily influenced by P_{FA}.

The situation for square-law detection is considerably less promising; in fact, it is doubtful that many would consider peak detection/holding worthwhile if only square-law detection were expected. However, displays are not normally developed for specific applications, and we conclude linear detection is probably the dominant case.

EXPERIMENTAL RESULTS

Figure 10 shows the peak detect/hold circuit, which uses digital techniques and functions as a black box inserted between a radar video output and a PPI display. It samples the video over a group of radar range cells corresponding to the display cell size, i.e., over ρ range cells, selects the largest sample in the group, and applies this signal to the display, thus covering approximately one display cell per peak detect/hold interval. The interval is operator selectable to allow matching for any combination of pulse width and sweep rate. The procedure can be automated, as shown later.

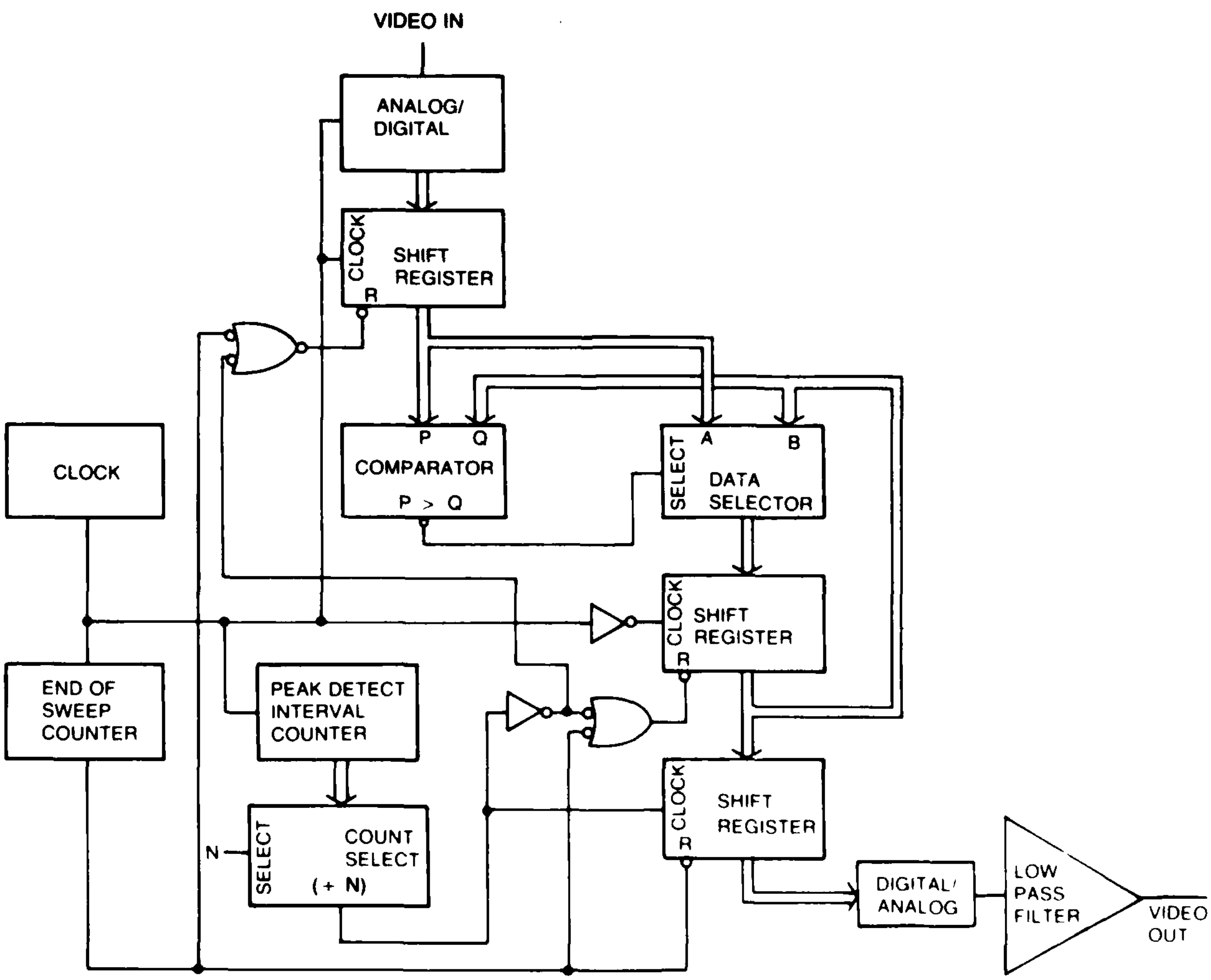

Fig. 10 — Peak select/hold circuit block diagram

The circuit of Fig. 10 selects the largest sample in the peak detect interval; this value is not necessarily the same as the peak value. We sample at a rate sufficient to preserve the video, i.e., about three samples per radar pulse width. The sampling loss is not considered significant. An alternate method would involve the use of an analog peak detect/hold circuit, which would provide the peak value. However, we found the first approach to be more expedient.

The AN/SPS-10 radar is known to incur L_c when operating at 0.25-μs pulse width in conjunction with an AN/SPA-25 PPI set up to display maximum instrumented range. Both were readily available at the CBD. An estimate of the AN/SPS-25 spot size was gained by applying a pulse train to the display's video input. If the pulse width is kept small, the pulse repetition frequency (PRF) can be varied to obtain a set of just-resolvable range rings where the width of each ring corresponds to the diameter of the spot. Thus, for a 10-in. display and 400 resolvable range rings, spot size is approximately

$$d \approx \frac{5 \text{ in.}}{400 \text{ rings}} = 0.0125 \frac{\text{in.}}{\text{ring}}.$$

Sweep speed is a function of displayed range. With a displayed range of 60 mi, sweep speed is approximately

$$s \approx \frac{5 \text{ in.}}{60 \text{ nmi} \times 12.3 \mu\text{s/nmi}} = 0.0068 \frac{\text{in.}}{\mu\text{s}}.$$

Figure 11 shows an HP-618C signal generator inserting a signal into the AN/SPS-10 receiver via its internal directional coupler. Figure 12 shows isolation of the pulse in the video displayed on an oscilloscope using a 0.2-μs/div time base. Pulse length on the PPI for this approximately 0.3 μs pulse (the shortest obtainable) is

$$sT_p \approx 0.0068 \frac{\text{in.}}{\mu\text{s}} \times 0.3 \mu\text{s} = 0.00204 \text{ in.}$$

Therefore, from Eq. (3),

$$\rho = \frac{d}{sT_p} \approx \frac{0.0125}{0.00204} = 6.1$$

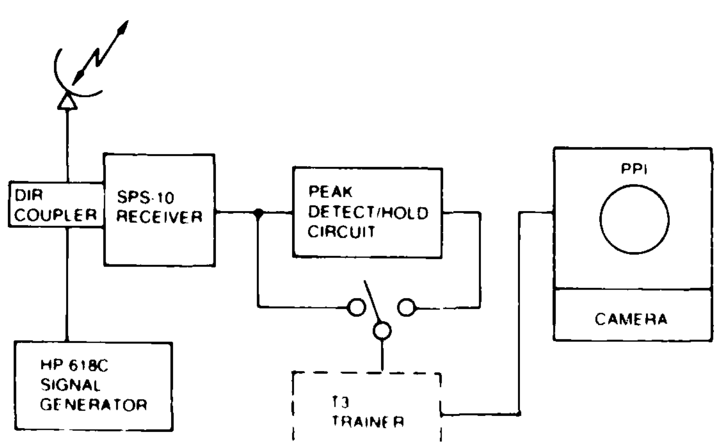

Fig. 11 Experimental set-up

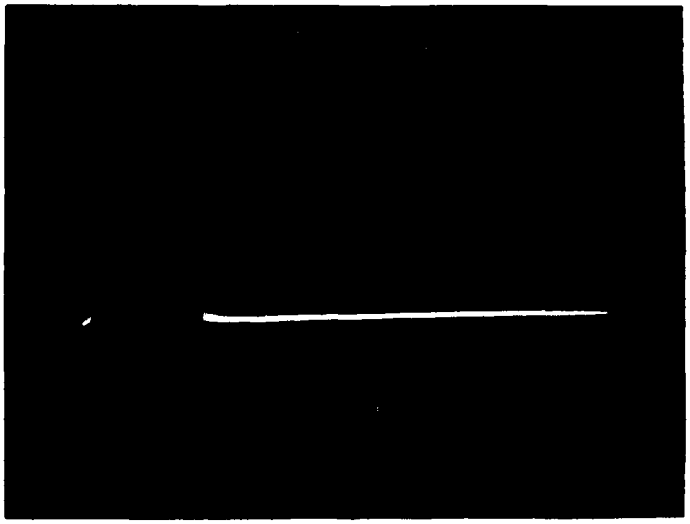

Fig. 12 — Pulse from HP-618c inserted in the video

Figure 13(a) shows the range ring obtained from the HP-618C inserted pulse train as it appears in the mismatched case; in Fig. 13(b) the improvement in detectability using the peak detection/hold circuit is apparent. Since the inserted signal from the HP-618C signal generator roughly corresponds to the 0.25-μs pulse width of the AN/SPS-10 radar, Figs. 13(a) and (b) are indicative of the improvement possible in detecting weak targets at long ranges. A fairly good resolution match (16 samples at approximately 10 MHz sampling rate equate to 1.6 μs $\times$ 0.0068 in./μs = 0.011 in. pulse duration vs 0.0125 in. estimated spot diameter) exists; in Fig. 13, two injected noise strobes 180° apart provide a background reference illustrating constant display gain for the two setups. Data from the simulation indicate the L_c to be about 5 to 6 dB for linear detection and about 2 to 2.5 dB for square-law detection in this situation, of which approximately 4 to 5 dB and 1 to 1.5 dB respectively, are recoverable with peak detection/holding. It is doubtful that 1 to 1.5 dB would provide the amount of improvement seen in the PPI photos. Therefore, we conclude that the detection process was linear in this region.

COLLAPSING RATIO IN CURRENT SHIPBOARD SYSTEMS

As previously indicated, maximum L_c occurs when the display scale is switched to the maximum instrumented range and the radar waveform is selected to provide the finest range resolution (it is assumed this combination is employed in sea operations). For example, with the maximum range set at 250 nmi on a SPA-25 display, an SPS-49 radar having a Mode 1 range resolution of 0.16 nmi has 250/0.16 = 1543 range cells over about 400 display-resolvable cells. Thus, one display cell contains about 1543/400 = 3.9 range cells with one of them containing signal and about three containing noise alone. Table 2 summarizes the situation for several different radars used with the SPA-25 stroke display, measured to have about 400 resolvable range rings. Figure 5 shows the above example corresponding to an L_c of about 4 dB in the raw video of which about 3.5 dB is theoretically recoverable through peak detection/holding.

It can be seen from these few examples that collapsing ratios vary in the range of approximately 1 to 10, which, as shown, can lead to collapsing losses up to 6 or 7 dB. A display, with a resolution that is coarser by a factor of two than the SPA-25 stroke display would increase the collapsing ratio to the range of 1 to 20 and the corresponding L_c to greater than 10 dB for linear detection. This could be the case with a raster scan display having an inadequate number of lines per frame.

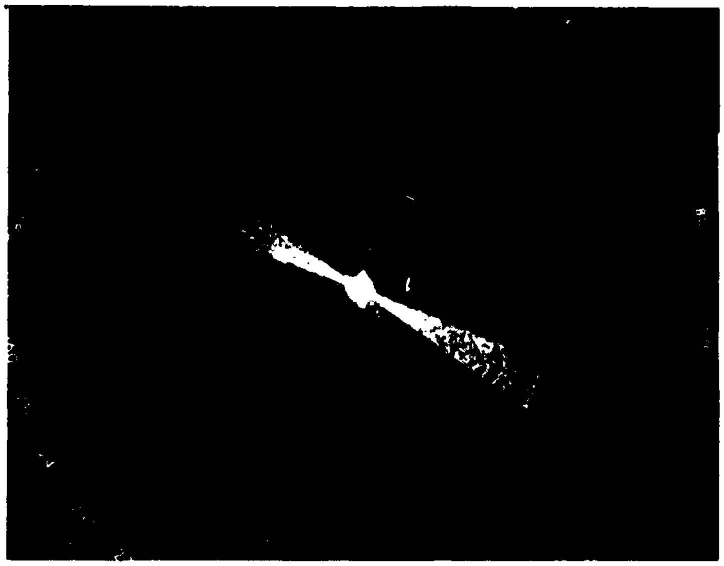

(a)

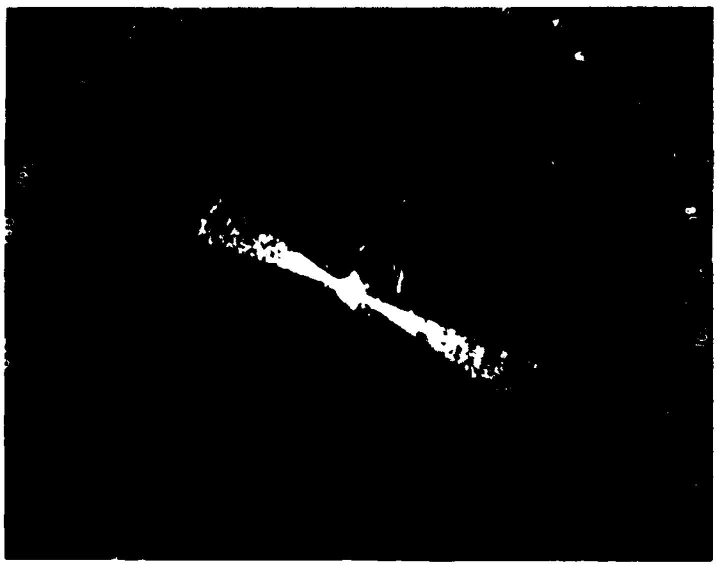

(b)

Fig. 13 — PPI photos showing (a) normal video and (b) improvement in detectability using peak detection/holding

Table 2 — Collapsing Ratio for Several Radars

Radar	Max. Range Setting on Display (nmi)	Range Resolution (nmi)	No. of Range Cells Over 400 Rings	No. of Range Cells per Display Cell (ρ)	Type Det
SPS-49 (MODE 1)	250	0.1600	1543	3.9	Coherent
BPS-15	32	0.0082	3902	9.6	Diode
SPS-10	60	0.0210	2854	7.1	Diode
SPS-67	32	0.0082	3902	9.6	Diode

The SPA-25 is representative of displays currently found aboard ship. As a class, they would be expected to experience L_c when used with long range search radars with compressed (or uncompressed) pulse widths on the order of a microsecond or with shorter range radars with submicrosecond pulsewidths. The peak detect/hold technique is believed to be incorporated into airborne radar systems such as the APS-116 and is suggested for shipboard use.

IMPLEMENTATION CONSIDERATIONS

If a radar and display are to be matched at all times the peak detect/hold interval will have to be made a function of displayed range, i.e., sweep speed. Displayed range is selected by the PPI operator and is a display function. Several displays (possibly mixed types) may be displaying the same video, but not set up for the same maximum range, or different videos (from the same or different radars). These facts support a conclusion that the peak detect/hold circuit should be a display function instead of a radar function. Thus, the requirement for matching from Eq. (3),

$$sT_p = d, \quad \rho = 1,$$

becomes

$$sT_{pd} = d, \quad \rho \geq = 1,$$

where T_{pd} is the required peak detect/hold interval. Hence,

$$T_{pd} = d/s, \tag{5}$$

and the peak detect/hold interval is inversely proportional to sweep speed. (Note that the peak detect/hold interval is a display-dependent parameter only and is independent of the radar pulse width, allowing the display to be associated with any radar through the usual switchboard arrangement and remain pseudo matched in each case.)

This analysis applies to a stroke display. For a raster display, the situation is essentially the same. In the usual scan-converter operation, the samples from the analog-to-digital (A/D) memory are mapped from an $r\theta$ (stroke) format to an xy (raster) format refresh memory. Sweep timing is necessary for this mapping process. Thus, for both stroke and raster displays a sweep speed parameter can be developed. This would most likely come from the setting of the range select control. However, a direct measurement with corresponding normalization is also possible.

The peak detect/hold method for reducing L_c in displays also has an associated range offset. Correction involves delaying the range zero trigger (T_m) to the display by the peak detect time interval. In Fig. 14(a), one method of obtaining a variable delay is provided to add completeness to the subject. Figure 14(b) shows a ROM-based approach for making the peak detect time interval a function of displayed range.

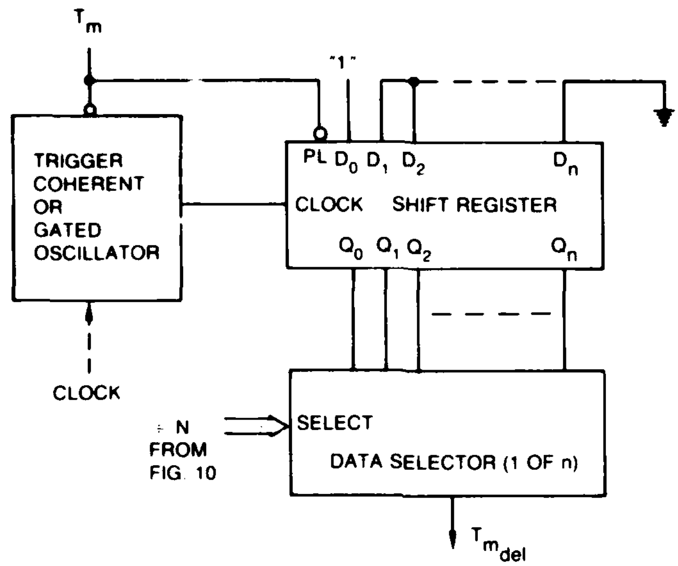

(a)

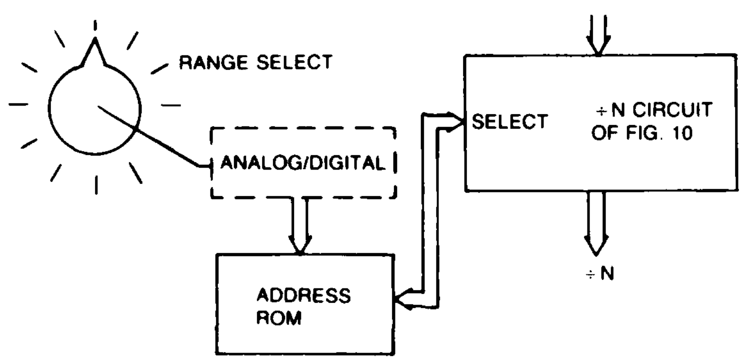

(b)

Fig. 14 — (a) Range offset correction circuit and (b) peak detect interval select circuit

An alternative that is not recommended but easier to implement, would be to provide an operator the capability to selectively employ a fixed time interval with an associated fixed offset correction. The operator would then use the circuit whenever conditions warranted it.

Parenthetically, note that synthetic video can be displayed without incurring the L_c that would normally be encountered for narrow pulses by selecting a pulse width more consistent with a representative spot size. However, a loss in resolution could result at the shorter ranges. A trade-off between resolution and L_c could perhaps be made so that some degradation could be accepted in both areas.

SUMMARY AND CONCLUSIONS

We have seen that a collapsing loss occurs when a radar and its associated display are mismatched, and that the maximum loss occurs when the display is set up to display maximum range. We have also shown that, for linear detection, the loss can be greatly reduced by employing peak detection/hold circuitry to obtain a pseudo resolution match between radar and display. The situation is not as favorable for square-law detection. The simulation data suggest that the loss can be held to about 1.5 dB (a 6 dB improvement) at a collapsing ratio of 10, about 1 dB (a 4 dB improvement) at a collapsing ratio of 5 for linear detection, and about 1.25 dB (2 dB improvement) and 0.75 dB (1.5 dB improvement) for square-law detection. These collapsing ratios are shown to be consistent with the situation existing in current shipboard systems. However, the peak detect/hold method has an associated range offset that should be compensated for, and, if the radar and display are to be matched at all times, the peak detect/hold interval must be made a function of displayed range.

The question of whether almost/barely visible signals on a display correspond more closely to a linear or square-law detection process is left open. The experimental data suggest it is linear. Some researchers, e.g., Blake [5], lead us to conclude it is probably linear. However, it may be linear in some radars and square law in others. In any event, additional investigation seems warranted.

Data were obtained for nonfluctuating targets, single-hit probability of detection, and at one P_{FA} (10^{-3}). Since some of the Navy's radars (the SPS-10 is not among them) include postdetection integration prior to PPI display, it would be worthwhile (especially for scan-converted displays) to investigate the effect of postdetection integration on L_c with and without peak detection/holding. The curves provided by Trunk [4] indicate postdetection integration would reduce L_c with linear detection and increase it with square-law detection. Study of the L_c phenomenon for cases other than Swerling Case 0 and at different P_{FA}s would provide completeness to the subject but is not expected to change the general character of the results.

The peak detect/hold method seems to be a promising means of alleviating the collapsing loss often found in displays, and we hope to consider ways of implementing it in Navy radar systems in the future. The AN/SPA-25 (G) scan-converted display currently in development appears to be one such candidate since NRL will have a test bed for this system at CBD.

REFERENCES

1. M.I. Skolnik, *Introduction to Radar Systems* (McGraw-Hill Book Co., New York, 1962).

2. D.P. Meyer and H.A. Mayer, *Radar Target Detection* (Academic Press, New York and London, 1973).

3. R. Payne-Scott, "The Visibility of Small Echoes on Radar PPI Displays," *Proc. IRE*, **36**, 180-196 (1948).

4. G.V. Trunk, "Comparison of the Collapsing Losses in Linear and Square Law Detectors," *IEEE Proc.* 743-744 (1972).

5. M.I. Skolnik, ed., *Radar Handbook* (McGraw-Hill Book Co., New York, 1970).

6. W.M. Waters and G.J. Linde, "Frequency-Agile Radar Signal Processing," *IEEE Trans. Aerosp. Electron. Syst.* **AES-15** (3), 459-464 (1979).

END
11-87
DTIC